JWMM

Long Memory, Time Trends, and the Degree of Persistence in Water Temperatures of Five European Rivers and Lakes

Luis A. Gil-Alana, María Jesús González-Blanch, Carmen Lafuente, Tiina Nõges and Merja Pulkkanen (2023)
University of Navarra, and Universidad Francisco de Vitoria; Universidad Francisco de Vitoria; Estonian University of Life Sciences; Finnish Environment Institute SYKE

DOI: https://doi.org/10.14796/JWMM.C505

ABSTRACT

This paper uses long memory and fractional integration techniques to analyze the presence of time trends in the water temperatures of three large European rivers (the Rhine at Lobith, the Danube at Wienna, the Meuse at Eijsden) and two lakes (Saimaa in Finland, and Võrtsjärv in Estonia). Long memory is a feature frequently observed in hydrological data, and it is important to consider it to appropriately estimate the potential trends in the data. The results indicate the existence of significant positive trends in all the five series examined, possibly as a consequence of global warming. Interestingly, once the time trends are taken into consideration, the degree of persistence substantially decreases in all cases and the long memory property in the data disappears.

1. INTRODUCTION

Among water quality characteristics, temperature appears to be the most significant. Most of the physical properties of water are functions of temperature. (Kothandaraman 1971). The main factor that determines the thermal regime of rivers (Wu et al. 2015) and lakes (Nõges and Nõges 2014; Schimd et al. 2014; O'Reilly et al. 2015; Piccolroaz et al. 2021) is air temperature (Edinger et al. 1968; Zabolotnia 2018; Kimura et al. 2021). Some

Gil-Alana, L.A., M.J. González-Blanch, C. Lafuente, T. Nõges, and M. Pulkkanen. 2023. "Long Memory, Time Trends, and the Degree of Persistence in Water Temperatures of Five European Rivers and Lakes." *Journal of Water Management Modeling* 31: C505. https://doi.org/10.14796/JWMM.C505
www.chijournal.org ISSN: 2292-6062

authors (Langan et al. 2001; Koycheva and Karney 2009) have calculated an increase of 0.3 to 0.9^{o} C in water temperature for every degree Celsius that air temperature increases.

Further, increased water temperature can result in marked changes in species composition and the functioning of aquatic ecosystems (Yang et al. 2021). Several researchers have reported that water temperature is considered to be a key variable in determining the overall health of fish and other aquatic organisms (Risley 1997; Karvonen et al. 2010; Piccolroaz et al. 2021).

Following the European Environment Agency study (EEA 2017), our study examines the presence of time trends in the water temperatures of five large European rivers and lakes over the last 100 years using fractional integration techniques.

To detect long-term persistence, or long memory, in hydrological data, researchers such as Iliopoulou et al. (2018) who studied the dependence structure of annual rainfall (according to Hurst-Kolmogorov behaviour, Hurst 1951) using a large dataset, comprising more than a thousand stations worldwide spanning 100 years or more, as well as a smaller number of paleoclimatic reconstructions covering the last 12,000 years. Gil-Alana (2009) examined the Australian annual average rainfall data for the period 1900-2006 using a statistical approach based on fractional integration with a structural break.

Addressing water temperatures in rivers and lakes, studies such as Lye and Lin (1994) analyzed the short- and long-term dependence of the peak flow series of 90 Canadian rivers. The results showed that although short-term dependence was practically absent for most of the series, significant long-term dependence was present for many of the tested peak flow series. Montanari et al. (2000) used a special form of the generalized ARFIMA (autoregressive fractionally integrated moving average) model on the Nile River monthly flows at Aswan to detect whether long memory was present. Later, Montanari and Rosso (1997) used an ARFIMA model to analyse short- and long-term persistence in the hydrologic time series of monthly and daily inflows of Lake Maggiore, Italy.

Corduas and Piccolo (2006) examined a model-based decomposition method, denoted as DECOMEL (Decomposition Methodology), for the estimation of the short memory and the long memory components of the river flow series. Montanari (2012) used graphical and analytical techniques to inspect the variability of the Po River flows and their persistence properties to gain a better understanding of natural patterns. Aguilar et al.(2017) analysed the memory properties of catchments for predicting the likelihood of floods based on observations of average flows in pre-flood seasons for the Po River and the Danube River.

Other studies used long-range dependence and fractional integration in hydrological data, such as Lohre et al. (2003) who used flexible seasonal long-memory models to study the water flow of the Rhine River.

In this context, Mudelsee (2007) examined the long memory feature on six European,

Asian, and African rivers, and proposed an explanation based on spatial aggregation of precipitation contributions to a river network. Also, Szolgayova et al. (2014) analysed long range dependence of river flows in Europe and its influencing factors. Furthermore, Maftei et al. (2016) studied long-range dependence (LRD) in the Taita River in Romania.

Recent studies such as Papacharalampous and Tyralis (2020) examined the hydrological time series forecasting using annual river flow time series for North America and Europe. These authors combined multiple methods such as simple exponential smoothing, complex exponential smoothing, and automatic autoregressive fractionally integrated moving average (ARFIMA).

Following this line of research, and in particular the abundant literature on long memory in hydrological series, this paper examines the long memory feature and the existence of linear trends in the water temperature of five large European rivers and lakes. Allowing this feature throughout fractional integration, we get more appropriate results about the estimation of trends in the data, not covered by the standard methodology that does not consider the possibility of fractional degrees of differentiation. We demonstrate the existence of significant positive trends in all the five series examined, possibly as a result of global warming.

2. STUDY AREA AND DATA

2.1 Study area

In this study, we use annual average water temperatures in the following rivers and lakes: Lake Võrtsjärv, Lake Saimaa. River Danube, Meuse River, and Rhine River.

Lake Võrtsjärv is in a shallow pre-glacial basin in the southern part of Estonia, centred around 58°17'N and 26°03'E. Water level (WL) is not regulated, at mean WL the lake area is 270 km^2, volume is 750 million m^3, mean depth is 2.8 m, and maximum depth is 6 m. The lake is ice-covered for an average of 131 days a year, commonly from the end of November to mid-April. The existence of a large area open to winds makes the lake highly sensitive to atmospheric drivers (Nõges and Nõges 2012).

Lake Saimaa is in the south-eastern part of Finland, centred around 61.33 N and 28.11 E. The surface temperature measurement station is located near the city of Lappeenranta in 61.04 N and 28.16 E. Lake Saimaa is the largest lake in Finland and it is regulated with a lake area of 1393 km^2, volume of 14.8 km^3, mean depth of 10.8 m, and a maximum depth of 85.8 m. During the period 1961-2000, Lake Saimaa was ice-covered for an average of 149 days (Finnish Environment Institute n.d.).

The Danube is the second largest river in Europe and drains an area of 801,093 km^2. The

Danube rises at the confluence of the Breg and Brigach rivers in the Black Forest near Donaueschingen (Germany) and flows for about 1770 miles (2850 km) to its mouth in the Black Sea. Along its course it passes through 10 countries: Germany, Austria, Slovakia, Hungary, Croatia, Serbia, Bulgaria, Romania, Moldova, and Ukraine (Sommerwerk et al. 2009; Pinka et al. 2022). There are three sections in the river basin: the upper course extends from its source to the gorge known as the Hungarian Gates, in the Austrian Alps and the Western Carpathians; the middle course runs from the Hungarian Gates Gorge to the Iron Gate in the Carpathians of southern Romania; and the lower course flows from the Iron Gate to the delta-shaped estuary in the Black Sea. Addressing the temperature of the river waters, the temperature is low in the upper reaches, where the summer waters derive from alpine snows and glaciers. In the middle and lower reaches, summer temperatures range between 22 and 24° C (71 and 75° F), while winter temperatures drop below freezing (Sommerwerk et al. 2009). The movement of goods is the most important economic use of the Danube. It is also used for hydroelectricity generation, industrial and residential water supply, irrigation, and fishing (Pinka et al. 2022).

The Meuse River is one of the most important waterways in Western Europe and is navigable for most of its length. The Meuse River rises at Pouilly on the Langres Plateau in France and flows generally northward for 590 miles (950 km) through Belgium and the Netherlands to the North Sea (Britannica 2014). The Meuse basin can be subdivided into three main geological zones: the Lotharingian Meuse (upstream of Charleville-Mézières), the Ardennes Meuse (between Charleville-Mézières and Liège) and the third zone is located downstream of Liège. The Dutch and Flemish lowlands are made up of unconsolidated sedimentary rocks from the Cenozoic. About 60% of the Meuse basin is used for agricultural purposes (including pasture) and 30% is covered in forests. Average annual precipitation ranges from 1000–1200 mm in the Ardennes to 700–800 mm in the Dutch and Flemish lowlands. The maximum altitude is just under 700 meters above sea level. Snowmelt is not a major factor in the discharge regime of the Meuse. (De Wit 2007).

The River Rhine is one of the great rivers of Europe, and one of the most important industrial transport arteries in the world. It flows from two small tributaries in the Alps of east-central Switzerland north and west through the Netherlands to the North Sea where it empties. With a total length of about 1230 km, it is generally navigable for about 540 miles (870 km), as far as Rheinfelden on the Swiss-German border. Its catchment area, including the delta area, exceeds 85,000 square miles (220,000 km^2). (Sinnhuber et al. 2023). Temperature and precipitation vary considerably with altitude and local topography. The mean annual temperature of the Rhine basin is 8.3^o C, 11.2^o C in the thermally favoured valley of the Upper Rhine, and 3000 m asl. Precipitation in the basin averages 945 mm/year (Uehlinger et al. 2009).

2.2 Data

The data have been provided by different sources: water temperature of Lake Võrtsjärv

comes from the Centre for Limnology at Estonian University of Life Sciences and from the Estonian Environment Agency; the water temperature of Lake Saimaa comes from the Finnish Environment Institute SYKE; the water temperature data of the Danube River have been provided by the Slovak Hydrometeorological Institute (Slovenský hydrometeorologický ústav), and the surface temperature in the rivers Rhine and Meuse were obtained from the Compendium of Environmental Data (CBS, PBL, RIVM, WUR 2020)

Annual data are used in the study and the series began in 1943 for the Danube, 1910 for the Meuse Rhine, 1916 for Saimaa (average water temperature in May-December, and average water temperature in the third trimester (July–September, 3T)), and 1952 for Võrtsjärv. The series ends in 2019 for the Meuse and Rhine, and in 2020 for the Danube and the two lakes (Table 1).

Table 1 Starting and ending years of analysed water temperature time series (annual data)

Series	Start	End	Number of observations
River Rhine, Lobith	1910	2019	110
River Danube, Vienna	1943	2020	78
River Meuse, Eijsden	1910	2019	110
Lake Saimaa, Finland	1916	2020	105
Lake Võrtsjärv, Estonia	1952	2020	69

3. METHODS

Using a methodology based on fractional integration, our study includes one important contribution, rather than imposing that the residuals of the detrended series are stationary *I(0)* (short memory) as is standard in the literature, we allow for long memory processes. In fact, we consider the possibility of long memory by allowing the errors to be fractionally integrated *I(d)*, where *d* is a fractional positive value. By estimating the fractional differencing parameter *(d),* we allow a much richer degree of flexibility in the dynamic specification of the model, including the standard *I(0)* specification as a case when $d = 0$. Moreover, in the context of testing for time trends, if the associated errors are not *I(0)* but *I(d)* with $d > 0$, the estimates of the trend coefficients will be clearly biased, producing erroneous conclusions about the water temperatures.

Long memory or long-range dependence is a special feature of the data whose observations are highly autocorrelated. Rigorously speaking, two definitions can be

provided for this concept, one in the time domain, and the other, in the frequency domain.

In the time domain, given a zero-mean covariance or second order stationary process $\{x_t, t = 0, \pm 1, ...\}$ with autocovariance function $E\left[\left(x_t - Ex_t\right)\left(x_{t-i} - Ex_t\right)\right] = \gamma_i$, we say that x_t displays long memory if the sum of the autocovariances is infinite, i.e.,

$$\lim_{T\to\infty} \sum_{j=-T}^{T} \left|\gamma_j\right| = \infty \tag{1}$$

Where:

T = sample size
γ_j = autocovariance function

Assuming that x_t has a spectral density function given by:

$$f(\lambda) = \frac{1}{2\pi} \sum_{j=-\infty}^{\infty} \gamma_j \cos\lambda, -\pi < \lambda \leq \pi \tag{2}$$

Where:

λ = frequency

Then, using the frequency domain, the spectral density function must be unbounded at some frequency λ in the interval *[0,* π*]*, i.e.,

$$f(\lambda) \to \infty, as\, \lambda \to \lambda^*,\ \lambda^* \in [0, \pi] \tag{3}$$

Where:

λ^* = a frequency point in the spectrum

(See McLeod and Hipel 1978). Long range dependence was introduced in hydrology by Hurst (1951), who observed the presence of this feature in the well-known series of annual minima storage of the Nile River.

There are many processes that satisfy the above two properties. One model is the Fractional Gaussian Noise (FGN) (Mandelbrot and Van Ness 1968). Another simple model, very popular among time series analysts, is the *I(d > 0)* or fractionally integrated, which is the one used in this application. A process $\{x_t, t = 0, \pm 1, ...\}$ is said to be integrated of order *d,* and denoted as *I(d)* if it can be represented as:

$$(1 - B)^d x_t = u_t, t = 0, \pm 1, ... \tag{4}$$

Where *B* is the backshift operator, i.e., $B^k x_t = x_{t-k}$, the parameter *d* can be any integer

or fractional value and the *d*-differenced process u_t is supposed to be *I(0)* (or short memory), defined for our purposes as a covariance or second order stationary process where the infinite sum of the autocovariances is finite. Examples of *I(0)* processes are the white noise case and the stationary and invertible AutoRegressive Moving Average (ARMA)-type of processes. Long Memory takes place if $d > 0$. Using the Binomial expansion, the polynomial $(1-B)^d$ in Equation (4) can be expressed for all real *d,*

$$(1-B)^d = \sum_{j=0}^{\infty} \binom{d}{j} (-1)^j B^j = 1 - dB + \frac{d(d-1)}{2} B^2 - \cdots \quad (5)$$

Where:

j = implicitly defined in the sum from 1 to ∞

and thus,

$$(1-B)^d x_t = x_t - dx_{t-1} + \frac{d(d-1)}{2} x_{t-2} - \cdots \quad (6)$$

implying that Equation (4) can be expressed as:

$$x_t = dx_{t-1} - \frac{d(d-1)}{2} x_{t-2} + \cdots + u_t \quad (7)$$

Thus, if *d* is fractional, the actual value of x_t depends on all its history, and the higher the value of *d,* the higher the degree of association between the observations.

4. RESULTS AND DISCUSSION

All average annual water temperature time series (Figure 1) show a clear increasing trend ranging from 1.6º C in Lake Võrtsjärv to 4.1º C in the third trimester in Lake Saimaa. The temperature increase in the rivers was 2.1º C in the Danube, 3.3º C in the Rhine, and 2.6º C in the Meuse.

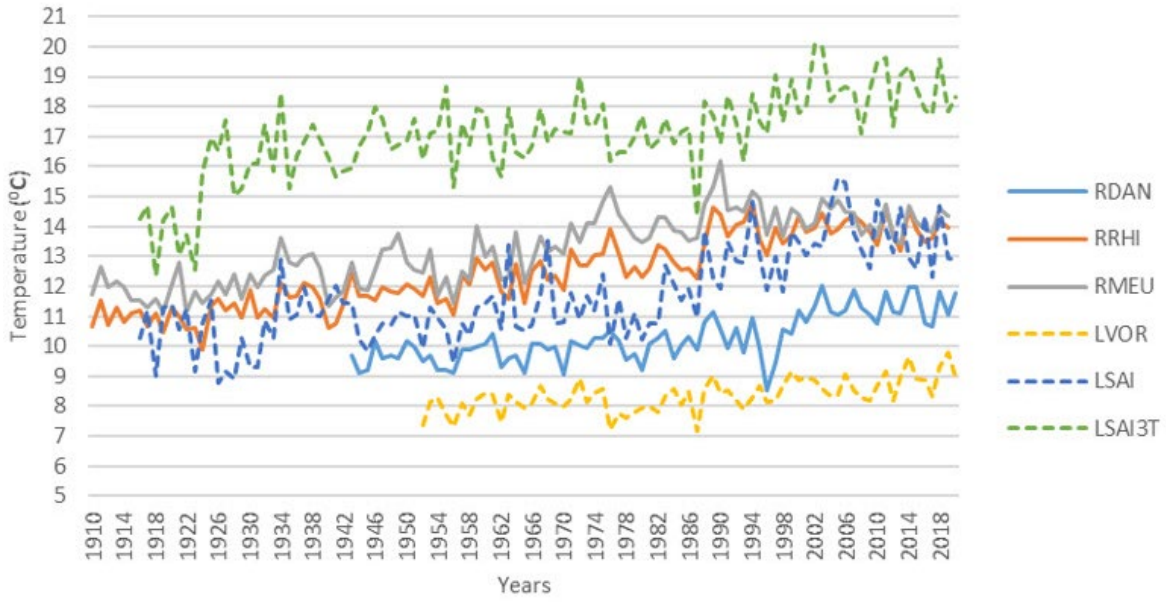

Figure 1 Annual average water temperature of large European rivers—Rhine (RRHI), Meuse (RMEU), Danube (RDAN), and lakes Võrtsjärv (LVOR) and Saimaa (May-December (LSAI) and in third trimester (LSAI3T)).

According to the EEA (2017), water temperatures have risen in European rivers and lakes in the range of 0.05 to 0.8° C per decade, with some cases of exceptional warming by more than 1° C per decade. Our study on the data of last four decades revealed temperature changes from -0.02° C to 1.99° C per decade with the strongest warming in the 1980s (Figure 2). During the first two decades of the twenty-first century, the behaviour of the series is irregular. The waters of the Danube River, the Meuse River, and Lake Võrtsjärv continued warming, while the temperatures dropped in the Rhine River and Lake Saimaa.

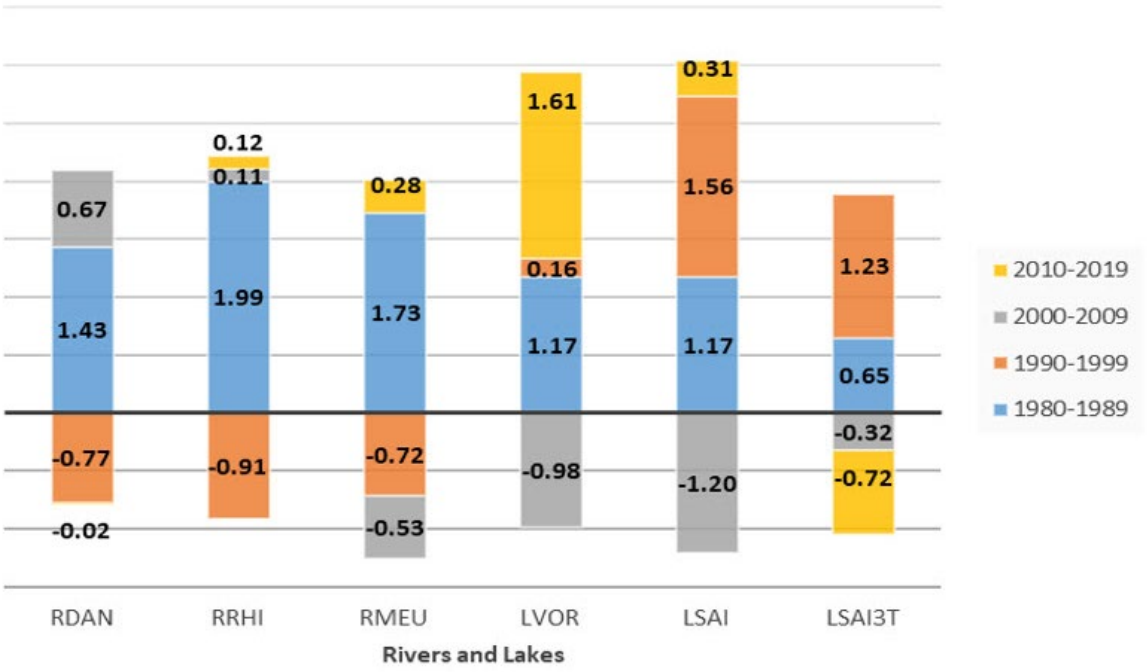

Figure 2 Accumulative temperature (sum year-on-year changes) for decades of large European rivers Rhine (RRHI), Meuse (RMEU) and lakes Võrtsjärv (LVOR) and Saimaa (LSAI).

To check if there are trends in the water temperatures, we consider the following model:

$$y_t = \beta_0 + \beta_1 t + x_t, t = 1, 2, \ldots \quad (8)$$

Where x_t is given by (4), i.e., showing a potentially fractionally integrated *I(d)* structure. In other words, the estimated model is:

$$y_t = \beta_0 + \beta_1 t + x_t, (1 - B)^d x_t = u_t, t = 1, 2, \ldots \quad (9)$$

Where:

y_t = observed time series,

β_0 and β_1 = coefficients corresponding to the intercept and the linear time trend, respectively, and

u_t = *I(0)*, specified in terms of an uncorrelated (white noise) process first, and then, allowing for weak dependence or weak autocorrelation.

The results displayed in Tables 2 and 3 focus on the uncorrelated errors, while those in Tables 4 and 5 refer to the autocorrelated case. Across the tables we display the results for three potential specifications: a) the case of no deterministic terms (i.e., $\beta_0 = \beta_1 = 0$ *a priori* in the undifferenced equation in (6)); b) including only a constant (β_0 unknown, and

$\beta_1 = 0$ *a priori*); and c) the case of a constant with a linear time trend (β_0 and β_1 unknown). The cases with significant coefficients have been marked in bold in Tables 2 and 4. *(These significant terms are determined by their corresponding t-values on the estimated coefficients.)*

Table 2 Estimates of *d* under no autocorrelation (white noise) errors

Series	No terms	An intercept	A linear time trend
LSAI	0.66 (0.54, 0.81)	0.39 (0.33, 0.47)	**0.21 (0.12, 0.35)**
LSAI3T	0.77 (0.66, 0.91)	0.34 (0.27, 0.43)	**0.21 (0.10, 0.35)**
Lake Võrtsjärv	0.87 (0.73, 1.07)	0.27 (0.16, 0.42)	**0.07 (-0.10, 0.32)**
River Danube	0.87 (0.73, 1.08)	0.41 (0.33, 0.56)	**0.25 (0.10, 0.48)**
River Meuse	0.89 (0.77, 1.06)	0.48 (0.42, 0.59)	**0.37 (0.24, 0.54)**
River Rhine	0.89 (0.76, 1.05)	0.48 (0.43, 0.56)	**0.17 (0.02, 0.38)**

In bold, the selected cases across the different three specifications for the deterministic terms. The values in parentheses refer to the 95% confidence bands for the estimated differencing parameter (d).

Table 3 Estimated coefficients in the selected models in Table 2

Series	*d* (95% band)	Intercept (t-value)	Time Trend (t-value)
Lake Saimaa	0.21 (0.12, 0.35)	9.883 (27.05)	0.0353 (6.16)
Lake Saimaa 3T	0.21 (0.10, 0.35)	5.026 (39.48)	0.0365 (6.11)
Lake Võrtsjärv	0.07 (-0.10, 0.32)	7.777 (63.47)	0.0166 (5.50)
River Danube	0.25 (0.10, 0.48)	9.297 (39.48)	0.0262 (5.26)
River Meuse	0.37 (0.24, 0.54)	11.724 (34.79)	0.0268 (5.06)
River Rhine	0.17 (0.02, 0.38)	10.627 (64.28)	0.0332 (13.34)

Starting with the case of uncorrelated errors, we observe in Table 2 that the time trend is statistically significant in the six cases examined, and the orders of integration are positive in all cases ranging from 0.07 (Lake Võrtsjärv) to 0.37 (River Meuse). For the former case, the *I(0)* hypothesis of short memory behaviour cannot be rejected, while for the rest of the cases, *d* is found to be significantly positive and thus displaying a long memory pattern. Also, it is worth noting that these results are very different to those reported in the second column of the table when no deterministic terms are included in the model. In this case, the orders of integration range between 0.66 and 0.89, implying large degrees of dependence and long memory behaviour. Thus, it seems that when the time trend is considered, there is a substantial reduction in the value of *d*, moving from nonstationary *($d \geq 0.50$)* to the stationary region *($d < 0.50$).* Table 3 displays the estimated coefficients for the deterministic terms, and we observe that the highest value

corresponds to Lake Saimaa (3T) (0.0365), followed by Lake Saimaa (0.0353) and the River Rhine (0.0332), while the lowest values, though still significantly positive, correspond to Lake Võrtsjärv (0.0166).

Next, we allowed a larger structure on the error term and permitted weak autocorrelation. However, instead of using a standard autoregressive moving average ARMA-type of process, we imposed here a non-parametric approach according to Bloomfield (1973), which is quite convenient in the context of fractional integration. It is non-parametric in the sense that there is no explicit functional form for the error term u_t), simply defined in terms of its spectral density function, which is given by:

$$f(\lambda;\tau) = \frac{\sigma^2}{2\pi} exp\left\{2\sum_{j=1}^{m}\tau_j \cos(\lambda j)\right\} \quad (10)$$

Where:

σ^2 = variance of the error term,

m = number of short run dynamics,

j = implicitly defined in the sum from 1 to *T, and*

τ_j = Chebyshev coefficients.

Bloomfield (1973) showed that given a stationary and invertible ARMA (*p, q*) process of form:

$$u_t = \sum_{r=1}^{p}\Phi_r u_{t-r} + \varepsilon_t + \sum_{s=1}^{q}\theta_s \varepsilon_{t-s} \quad (11)$$

Where:

p and q = orders of the AR and MA parts, respectively,

Φ_r and θ_s = AR and MA coefficients, respectively, and

ε_t = white noise process.

ε_t is a white noise process, whose spectral density function is given by:

$$f(\lambda;\tau) = \frac{\sigma^2}{2\pi}\left|\frac{1+\sum_{s=1}^{q}\theta_s e^{i\lambda s}}{1-\sum_{r=1}^{p}\Phi_r e^{i\lambda r}}\right|^2 \quad (12)$$

This latter expression could be very well approximated by (7) when p and q were small values. In the same way as with the stationary AutoRegressive (AR) model, this approach has autocorrelations that decay exponentially and thus, using this specification, we do not need to rely on as many parameters as in the AR case, which always results in being tedious in terms of estimation, testing, and model specification. Moreover, this model is stationary across all its parameters, unlike what happens with the AR models, and performs adequately well in the context of fractional integration (Gil-Alana 2004).

Table 4 Estimates of *d* under autocorrelation (Bloomfield 1973) errors.

Series	No terms	An intercept	A linear time trend
Lake Saimaa	0.76 (0.51, 1.08)	0.56 (0.44, 0.74)	**0.36 (0.15, 0.67)**
Lake Saimaa 3T	0.82 (0.63, 1.08)	0.41 (0.29, 0.58)	**0.34 (0.09, 0.60)**
Lake Võrtsjärv	0.88 (0.59, 1.23)	0.17 (-0.03, 0.38)	**-0.20 (-0.54, 0.19)**
River Danube	0.79 (0.51, 1.19)	0.40 (0.25, 0.57)	**0.06 (-0.18, 0.38)**
River Meuse	0.87 (0.62, 1.18)	0.54 (0.44, 0.71)	**0.33 (0.09, 0.69)**
River Rhine	0.85 (0.62, 1.15)	0.53 (0.46, 0.63)	**-0.08 (-0.26, 0.32)**

In bold, the selected cases across the different three specifications for the deterministic terms. The values in parentheses refer to the 95% confidence bands for the estimated differencing parameter (d).

Table 5 Estimated coefficients in the selected models in Table 4.

Series	*d* (95% band)	Intercept (t-value)	Time Trend (t-value)
Lake Saimaa	0.36 (0.15, 0.67)	10.031 (17.47)	0.0336 (3.59)
Lake Saimaa 3T	0.34 (0.09, 0.60)	14.808 (25.61)	0.0385 (4.12)
Lake Võrtsjärv	-0.20 (-0.54, 0.19)	7.792 (108.64)	0.0158 (8.25)
River Danube	0.06 (-0.18, 0.38)	9.246 (54.35)	0.0265 (7.21)
River Meuse	0.33 (0.09, 0.69)	11.709 (34.72)	0.0271 (5.23)
River Rhine	-0.08 (-0.26, 0.32)	10.562 (82.71)	0.0342 (16.67)

We observed that the time trend coefficient was again required in the six series, and the I(0) hypothesis could not be rejected in the cases of Lake Võrtsjärv, the River Rhine, and the River Danube, since the confidence intervals include the value 0 in these three series (Table 4). For the remaining three series (the River Meuse, Lake Saimaa, and Lake Saimaa 3T), the estimated values of d are significantly positive: 0.33 for the River Meuse; 0.34 for Lake Saimaa 3T, and 0.36 for Lake Saimaa. Like the previous case of white noise disturbances, there is a substantial reduction in the estimated value of d once the time trend is considered. Focusing on the time trend coefficients (Table 5), we see that the highest value corresponds again to Lake Saimaa 3T (0.0385), followed by the River Rhine (0.0342), Lake Saimaa (0.0336), the River Meuse (0.0371), the River Danube (0.0265), and Lake Võrtsjärv (0.0158).

5. CONCLUSIONS

This paper analyzes the water temperatures in five European rivers and lakes, the rivers Rhine at Lobith, Danube at Wienna, Meuse at Eijsden, and the lakes Saimaa (Finland), and Võrtsjärv (Estonia). The main objective was to determine if the series display long memory patterns and significant time trend coefficients, which may be related to the global warming hypothesis. Using fractionally integrated methods, the first noticeable feature was the substantial reduction observed in the degree of integration if the time trends were considered. In fact, if no trends are assumed, the series display a long memory pattern, with a high degree of integration, very close to the unit root case. However, if a linear time trend is imposed in the model, first we observe that the coefficients are significantly positive in the six series examined, which may be a consequence of global warming, and the orders of integration are now close to zero in practically all cases, implying short memory or close to short memory behaviour. Our results are also robust to the specification of the error term and indicate that random shocks in the series will have transitory effects, disappearing relatively fast and returning to their underlying trends sometime in the future.

DATA AVAILABILITY STATEMENT

Data are available at https://www.eea.europa.eu/data-and-maps/daviz and from the authors upon request. They are being archiving at the repository 4TU. Centre for Research Data.

ACKNOWLEDGMENTS

Luis A. Gil-Alana gratefully acknowledges financial support from the Grant PID2020-113691RB-I00 funded by MCIN/AEI/ 10.13039/501100011033. An internal project from the Universidad Francisco de Vitoria is also acknowledged.

REFERENCES

Aguilar, C., A. Montanari, and M.J. Polo. 2017. “Real-time updating of the flood frequency distribution through 515 data assimilation”. *Hydrology and Earth System Science* 21 (7): 3687-3700. https://doi.org/10.5194/hess-21-3687-2017

Bloomfield, P. 1973. “An exponential model in the spectrum of a scalar time series”. *Biometrika* 60 (2): 217-226. https://doi.org/10.1093/biomet/60.2.217

Britannica, T. Editors of Encyclopaedia. 2014. "Meuse River". *Encyclopedia Britannic*a, Accessed 27 March 2023 https://www.britannica.com/place/Meuse-River

CBS, PBL, RIVM, WUR. 2020. “Temperatuur oppervlaktewater, 1910–2019 (indicator 0566, versie 05, 22 december 2020).” Accessed 16 February 2022. https://www.clo.nl/indicatoren/nl0566-temperatuur-opervlaktewater?ond=20900

Corduas, M., and D. Piccolo. 2006. “Short and long memory unobserved components in hydrological time series”. *Physical Chemical and Earth Sciences* 31 (18): 1099-1106. https://doi.org/10.1016/j.pce.2006.01.013

De Wit, M.J.M., H.A. Peeters, P.H. Gastaud, P. Dewil, K. Maeghe, and J. Baumgart. 2007. “Floods in the Meuse basin: event descriptions and an international view on ongoing measures.” *International Journal of River Basin Management* 5 (4): 279–292.

Edinger, J.E., D.W. Duttweiler, and J.C. Geyer. 1968. “The Response of Water Temperature to Meteorological Conditions.” *Water Resources Research* 4 (5): 1137–1143.

European Environment Agency (EEA). 2017. “Climate change, impacts, and vulnerability in Europe 2016. An indicator-based-report.” Publications Office. https://doi.org/10.2800/534806

Finnish Environment Institute. (n.d). Environmental Data. Accessed 03 April 2023. https: //www.syke.fi/en-US/Open_information/Open_web_services/Environmental_data_API# Hydrology

Gil-Alana, L.A. 2004. “The use of the Bloomfield model as an approximation to ARMA processes in the context of fractional integration.” *Mathematical and Computer Modelling* 39 (4–5): 429–436. https://doi.org/10.1016/S0895-7177(04)90515-8

Gil-Alana, L.A. 2009. “Modelling Australian annual mean rainfall data: A new approach based on fractional integration.” *Australian Meteorological and Oceanographic Journal* 58: 119–128. https://doi.org/10.22499/2.5802.004

Hurst, H.E. 1951. “Long term storage capacity of reservoirs.” *Transactions of the American Society of Civil Engineers* 116 (1): 778–808. https://doi.org/10.1061/TACEAT.0006518

Iliopoulou, T., S.M. Papalexiou, Y. Markonis, and D. Koutsoyiannis. 2018. “Revisiting long-range dependence in annual precipitation. *Journal of Hydrology* 556: 891–900. https://doi.org/10.1016/j.jhydrol.2016.04.015

Karvonen, A., P. Rintamäki, J. Jokela, and E.T. Valtonen. 2010. “Increasing water temperature and disease risks in aquatic systems: Climate change increases the risk of some, but not all, diseases.” *International Journal for Parasitology* 40 (13): 1483–1488. https://doi.org/10.1016/j.ijpara.2010.04.015

Kimura, N., K. Ishida, and D. Baba. 2021. “Surface Water Temperature Predictions at a Mid-Latitude Reservoir under Long-Term Climate Change Impacts using a Deep Neural Network Coupled with a Transfer Learning Approach.” *Water* 13 (8): 1109. https://doi.org/10.3390/w13081109

Kothandaraman, V. 1971. “Analysis of water temperature variations in large rivers.” *ASCE Journal of the Sanitary Engineering Division* 97 (1): 19–31. https://doi.org/10.1061/JSEDAI.0001242

Koycheva J., and B. Karney. 2009. “Stream water temperature and climate change -An ecological perspective.” *International Symposium on Water Management and Hydraulic Engineering* A112, 771–777.

Langan, S.J., U.L. Johnston, M.J. Donaghy, A.F. Youngson, D.W. Hay, and C. Soulsby. 2001. “Variation in river temperatures in an upland stream over a 30-year period.” *The Science of the Total Environment* 265 (1-3): 195-207. https://doi.org/10.1016/S0048-9697(00)00659-8

Lohre, M., P. Sibbertsen, and T. Konnig. 2003. “Modeling water flow of the Rhine River using seasonal long memory.” *Water Resources Research* 39 (5): 1132. https://doi.org/10.1029/2002WR001697

Lye, L.M., and Y. Lin. 1994. “Long-term dependence in annual peakflows of Canadian rivers.” *Journal of Hydrology* 160 (1–4): 89–103. https://doi.org/10.1016/0022-1694(94)90035-3

Maftei, C., A. Barbulescu, and A.A. Carsteanu. 2016. “Long range dependence in the time series of the Taita River discharges.” *Hydrological Science Journal* 61 (9): 1740–1747. https://doi.org/10.1080/02626667.2016.1171869

Mandelbrot, B.B., and J.W. Van Ness. 1968. “Fractional Brownian motions, fractional noises and applications.” *SIAM Review* 10 (4): 422–437. https://doi.org/10.1137/1010093

McLeod, A.I., and K.W. Hipel. 1978. “Preservation of the rescaled adjusted range. A reassessment of the Hurst phenomenon.” *Water Resources Research* 14 (3): 491–507. https://doi.org/10.1029/WR014i003p00491

Montanari, A., and R. Rosso. 1997. “Fractionally differenced ARIMA models applied to hydrologic time series. Identification, estimation, and simulation.” *Water Resources Research* 33 (5): 1035–1044. https://doi.org/10.1029/97WR00043

Montanari, A., R. Rosso, and M.S. Taqqu. 2000. “A seasonal fractional ARIMA model applied to the Nile River monthly flows at Aswan.” *Water Resources Research* 36 (5): 1249–1259. https://doi.org/10.1029/2000WR900012

Montanari, A. 2012. “Hydrology of the Po River: Looking for changing patterns in river

discharge." *Hydrology and Earth System Sciences* 16 (10): 3739–3747. https://doi.org/10.5194/hess-16-3739-2012

Mudelsee, M. 2007. "Long memory of rivers from spatial aggregation." *Water Resources Research* 43 (1). https://doi.org/10.1029/2006WR005721

Nõges, P., and T. Nõges. 2012. "Võrtsjärv Lake in Estonia". In: *Encyclopedia of Lakes and Reservoirs*, L. Bengtsson, R.W. Herschy, R.W. Fairbridge (eds.). Springer, Dordrecht. 850-861. https://doi.org/10.1007/978-1-4020-4410-6_228

Nõges, P., and T. Nõges. 2014. "Weak trends in ice phenology of Estonian large lakes despite significant warming trends." *Hydrobiologia* 731: 5–18. https://doi.org/10.1007/s10750-013-1572-z

O'Reilly, C.M., S. Sharma, D.K. Gray, S.E. Hampton, J.S. Read, R.J. Rowley, P. Schneider, et al. 2015. "Rapid and highly variable warming of lake surface waters around the globe." *Geophysical Research Letters* 42 (24): 10,773–10,781. https://doi.org/10.1002/2015GL066235

Papacharalampous, G., and H. Tyralis. 2020. "Hydrological time series forecasting using simple combinations: Big data testing and investigations on one-year ahead river flow predictability." *Journal of Hydrology* 590: 125205. https://doi.org/10.1016/j.jhydrol.2020.125205

Piccolroaz, S., S. Zhu, M. Ptak, M. Sojka, and X. Du. 2021. "Warming of lowland Polish lakes under future climate change scenarios and consequences for ice cover and mixing dynamics." *Journal of Hydrology: Regional Studies* 34: 100780. https://doi.org/10. 1016/j.ejrh.2021.100780

Pinka, P.G., and P.G. Penčev. 2022. "Danube River." *Encyclopedia Britannica*. Accessed 27 March 2023. https://www.britannica.com/place/Danube-River

Risley, J.C. 1997. "Relations of Tualatin River water temperatures to natural and human-caused factors." *USGS Water-Resources Investigations Report* 97-4071: 143.

Schmid, M., S. Hunziker, and A. Wüest. 2014. "Lake surface temperatures in a changing climate: a global sensitivity analysis." *Climatic Change* 124: 301–315. https://doi.org/10.1007/s10584-014-1087-2

Sinnhuber, K.A., and A.F.A. Mutton. 2023. "Rhine River". *Encyclopedia Britannica*. Accessed 27 March 2023. https://www.britannica.com/place/Rhine-River

Sommerwerk, N., M. Schneider-Jajoby, C. Baumgartner, M. Ostojic, M. Paunovic, J. Bloesch, R. Siber, and K. Tockner. 2009. "The Danube River Basin." In: *Rivers of Europe*, K. Tockner, C.T. Robinson, U. Uehlinger (Eds.), Elsevier Ltd., London, UK, 59–113.

Szolgayova, E., G. Laacha, G. Bloschl, and C. Bucher. 2014. "Factors influencing long range dependence in streamflow of European rivers." *Hydrological Processes* 28 (4): 1573–1586. https://doi.org/10.1002/hyp.9694

Uehlinger, U.F., K.M. Wantzen, R.S. Leuven, and H. Arndt. 2009 "The Rhine River Basin" In: *Rivers of Europe*, K. Tockner, ed. London: Academic Press, 199–245.

Wu, W., K. Yoshiyama, and M. Senge. 2015. “Atmospheric conditions, landscape characteristics, and anthropogenic factors affecting stream water temperature.” *Reviews in Agricultural Science* 3: 46–53. https://doi.org/10.7831/ras.3.46

Yang, D., H. Park, A. Peterson, and B. Liu. 2021. “Arctic River water temperatures and thermal regimes.” In *Arctic Hydrology, Permafrost and Ecosystem: Linkages and Interactions*, D. Yang, and D. Kane. editors. Springer Nature 287–313. https://doi.org/10.1007/978-3-030-50930-9_10

Zabolotnia, T. 2018. “Estimation of the long-term tendencies and homogeneity of the average annual water temperature and air temperature in the Siverskyi Donets river basin (within Ukraine).” *Journal of Fundamental and Applied Sciences* 10 (2): 1–22.

APPENDIX

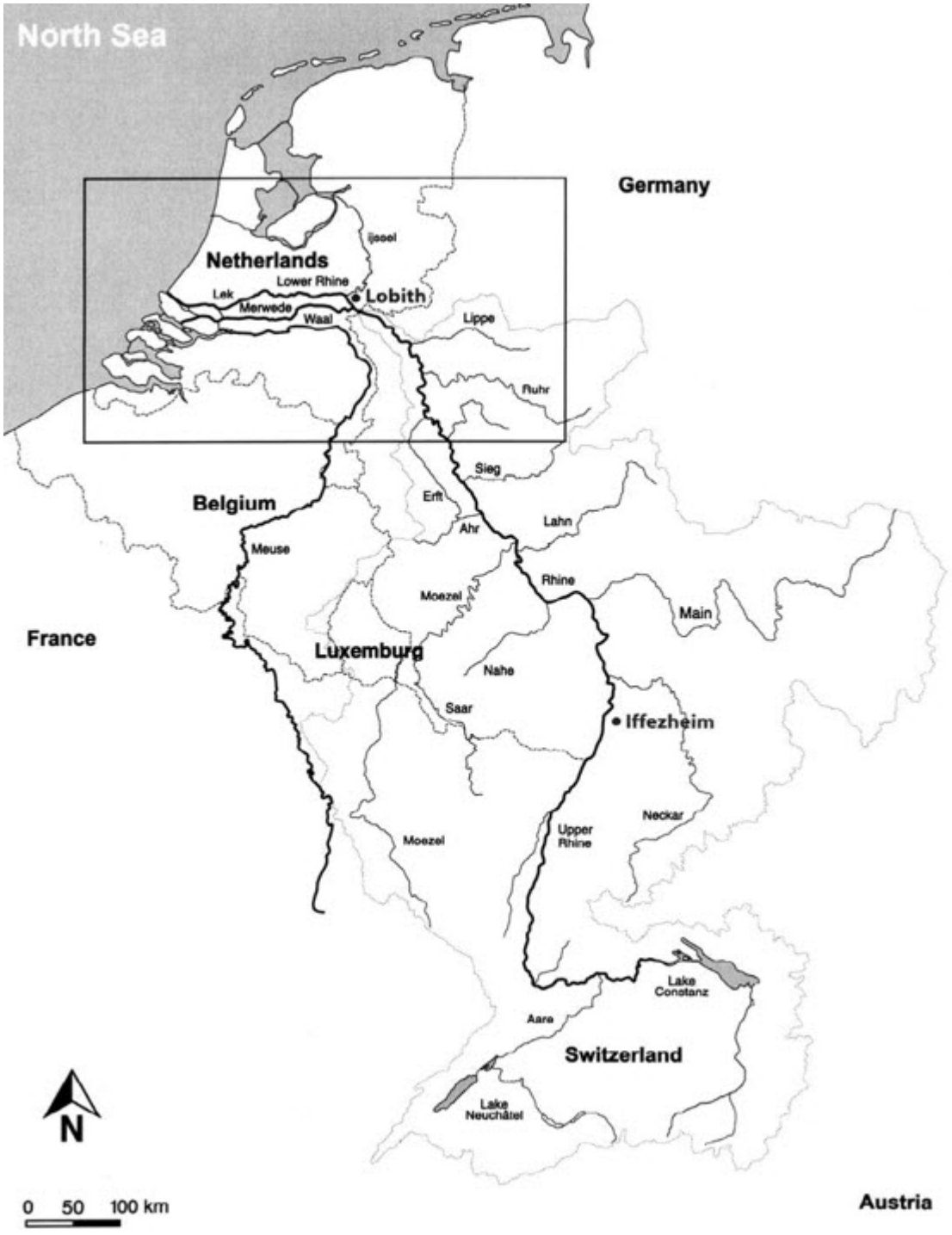

Figure A1 Rhine River and Meuse River

Source: https://www.researchgate.net/figure/The-catchment-of-the-river-Rhine-and-its-tributaries-The-Rhine-enters-the-Netherlands-at_fig2_227282622

Figure A2a Danube River

Source: https://www.researchgate.net/figure/The-map-of-Slovakia-with-topography-and-the-main-river-system-The-Zitn-yZitn-y-ostrov-is_fig1_258643118

Figure A2b Danube River

Source: https://worldinmaps.com/rivers/danube/

Figure A3 Lake Võrtsjärv

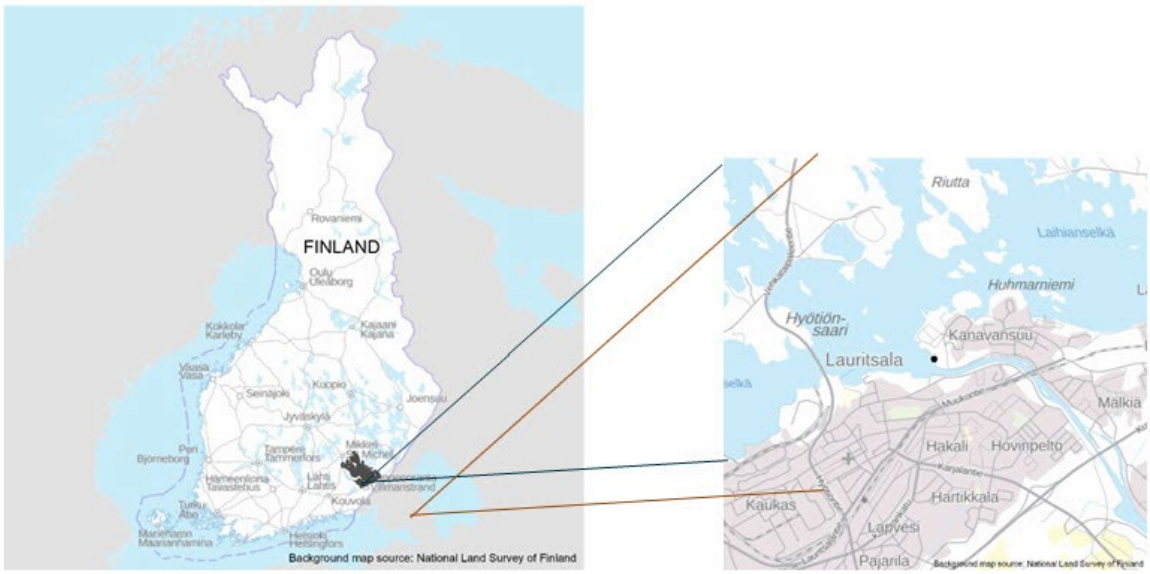

Figure A4 Location of Lake Saimaa in Finland
(Location of the surface water temperature measurement site)